Applied Catalysis B: Environmental 96 (2010) 508–515

Contents lists available at ScienceDirect

Applied Catalysis B: Environmental

journal homepage: www.elsevier.com/locate/apcatb

Transesterification of tributyrin with methanol over basic Mg:Zr mixed oxide catalysts

Joseph T. Kozlowski, Matthew T. Aronson, Robert J. Davis*

Department of Chemical Engineering, University of Virginia, 102 Engineers' Way, Charlottesville, VA 22904, United States

ARTICLE INFO

Article history:
Received 17 November 2009
Received in revised form 17 February 2010
Accepted 8 March 2010
Available online 15 March 2010

Keywords:
Base catalysis
Transesterification
Carbon dioxide microcalorimetry
Methanol
Tributyrin
IR spectroscopy

ABSTRACT

Two series of Mg:Zr mixed oxides, prepared by either co-precipitation or sol–gel synthesis, were characterized and evaluated in the base catalyzed transesterification of tributyrin with methanol. A co-precipitated Mg-rich mixed oxide catalyst with Mg:Zr 11:1 was approximately 300% more active than MgO on a surface area basis, whereas pure ZrO_2 was inactive for the reaction. To explore the nature of the activity enhancement, samples were characterized by X-ray diffraction, N_2 adsorption, CO_2 adsorption microcalorimetry and DRIFTS of adsorbed CO_2 and CH_3OH. Although the sol–gel synthesis method provided better atomic level mixing of Mg and Zr, the resulting catalysts were not as effective as mixed oxides prepared by co-precipitation. The most active mixed oxide (Mg:Zr 11:1) exhibited a high initial heat of CO_2 adsorption and modified modes of methanol adsorption compared to MgO. However, the CO_2 adsorption capacity did not correlate to catalyst activity.

1. Introduction

Many different alternatives are being explored to reduce the use of fossil fuels for energy generation and thereby reduce the addition of carbon dioxide to the atmosphere. One of the alternatives for transportation fuel is biodiesel, the common name for fatty acid methyl esters derived from naturally-occurring triglycerides. In one common process to produce biodiesel, triglycerides are transesterified with a short chain alcohol such as methanol to produce monoalkyl esters (biodiesel) and glycerol. The production of biodiesel is generally catalyzed by a homogeneous base catalyst such as sodium methoxide, sodium hydroxide, or potassium hydroxide [1–5]. Due to the separation requirements imposed on production systems that use homogeneous base catalysts, the search for a suitable solid base catalyst is being pursued [5–9]. Metal oxides represent solid catalysts with a high potential for replacing liquid catalysts [1–3,5]. Some metal oxides exhibit surface basic properties and high thermal stability, which makes them useful as solid base catalysts and catalyst supports [6,7,10]. Since the transesterification reaction is well-recognized to be catalyzed by solid bases, it serves as an excellent probe reaction for interrogating the nature of metal oxide surfaces [4,8,9,11].

Magnesia is a well-studied solid base metal oxide that catalyzes a variety of reactions, such as 2-propanol decomposition [12–14], Meerwein–Ponndorf–Verley reaction [15], methylbutynol decomposition [16], double bond isomerization [13,17], cycloaddition of CO_2 to epoxides [18], and transesterification [8]. Zirconia is of particular interest in this study because it is an amphoteric oxide that exposes both acid and base sites. Indeed, the transesterification of triglycerides occurs in the presence of basic and acidic catalysts, however the rate is orders of magnitude faster with a base catalyst [3–5,19]. Zirconia catalyzes a wide variety of reactions, such as dehydration and dehydrogenation of alcohols, conversion of synthesis gas to higher alcohols, hydrogenation of olefins, as well as hydrocracking, esterification and oxidation reactions [20]. A more complete discussion of the reactions catalyzed by zirconia can be found in Yamaguchi's review article [20].

Recent reports in the literature suggest that mixed oxides of Mg and Zr may exhibit desirable basic properties. The mixed oxide catalysts have been shown to expose more base sites than MgO based on temperature programmed desorption (TPD) of carbon dioxide and high activity for base catalyzed reactions, including 2-propanol to propanone [12,21], 2-methyl-3-butyn-2-ol decomposition [16], transesterification [22], Knoevenagel condensation [23] and bifunctional aldol condensations [24,25]. The nature of the mixed oxide catalysts appears to be affected by their synthesis method. Prior studies have utilized samples prepared by sol–gel chemistry, precipitation and impregnation [16,21,26–30].

In this particular study, several basic mixed oxides of magnesium and zirconium were synthesized, characterized and evaluated

* Corresponding author at: Department of Chemical Engineering, University of Virginia, 102 Engineers' Way, PO Box 400741, Charlottesville, VA 22904, United States. Tel.: +1 434 924 6284; fax: +1 434 982 2658.
E-mail address: rjd4f@virginia.edu (R.J. Davis).

0926-3373/$ – see front matter © 2010 Elsevier B.V. All rights reserved.
doi:10.1016/j.apcatb.2010.03.012

for activity in transesterification of tributyrin with methanol, a model reaction for biodiesel synthesis. A comparison of samples prepared by co-precipitation and by a sol–gel method will be presented. The surface character of the basic oxides has been explored by adsorption of probe molecules. In particular, Diffuse Reflectance Infrared Fourier Transform Spectroscopy (DRIFTS) of adsorbed carbon dioxide and methanol along with carbon dioxide adsorption microcalorimetry were used in this work.

2. Experimental methods

2.1. Catalyst preparation

2.1.1. Precipitation method

The following method, which we will refer to as precipitation or co-precipitation, was used to prepare pure metal oxide or mixed metal oxide, respectively, based on the work of Aramendía et al. [26]. First, 51 g of magnesium nitrate hexahydrate (Acros Organics, 98%) was dissolved in 1 l of deionized water. Zirconyl nitrate hydrate (Acros Organics, 99.50%) was also dissolved in the solution. The amount dissolved depended on the amount of zirconia desired in the catalyst. For example, to prepare a sample with a 11:1 molar ratio of Mg to Zr, 4 g of zirconyl nitrate hydrate was dissolved. The oxide was then precipitated by the dropwise addition of 25 wt.% NaOH solution (Mallinckrodt Chemicals, 98.8%). Sodium hydroxide solution was added until the metal oxide solution reached a pH of 10. The mixture was then allowed to age for 72 h, after which it was filtered and dried at 413 K. Subsequently, the catalyst was calcined at 773 K in 100 cm^3 min^{-1} of flowing ultra high purity dioxygen (GT&S Welco) for 3 h. After calcination, the catalyst was washed with 20 l of deionized water to remove adsorbed sodium. Catalysts prepared by this precipitation method will be denoted with -P after the catalyst descriptor, such as MgO-P and ZrO_2-P.

A mixed oxide of Mg and Ti was prepared using TiO_2 (Riedel-de Haen, puriss) as the precursor and was mixed into the solution containing magnesium nitrate. The magnesium was then precipitated onto the titania and calcined using the same procedure as described as above.

2.1.2. Sol–gel synthesis method

The sol–gel procedure was adapted from the work of Liu et al. [29]. Magnesium acetate tetrahydrate (Fisher Chemical, 99.2%) 0–80 g, was dissolved in 304 g of absolute ethanol (Sigma–Aldrich >99.5% ACS reagent), together with the non-ionic surfactant Pluronic P-123 (BASF). A solution containing 0–25 cm^3 of zirconium (IV) propoxide (70 wt.% in 1-propanol, Aldrich) and corresponding amounts of acetylacetone (Sigma–Aldrich ReagentPlus, >99%) 0–2.5 cm^3 was added to the ethanol solution, based on the amount of zirconium (IV) propoxide used. This mixture was stirred for 1 h at room temperature and then heated to 323 K, at which point 18 g of deionized water was added dropwise. The mixture was then held at 323 K for 24 h. The resulting slurry was filtered and the recovered solid was refluxed in 500 cm^3 of ammonium hydroxide solution at a pH 10 for 24 h at 373 K. The solid was again removed from solution by filtration. The material was dried in air at 413 K and then calcined by heating at 1 K min^{-1} to 973 K in flowing air at 100 cm^3 min^{-1}. Catalysts prepared by this sol–gel method will be denoted with -SG after the catalyst descriptor, such as MgO-SG and ZrO_2-SG.

For comparison, a mixed oxide of 3:1 Mg:Ti was prepared using titanium (IV) propoxide (Fluka) as the metal precursor and was treated exactly as above.

2.2. Catalyst characterization

The elemental analysis (Zr, Mg, Na) was performed by Galbraith Laboratories (2323 Sycamore Drive, Knoxville, TN 37921) using ICP-OES analysis.

Adsorption of N_2 was performed on a Micromeritics ASAP 2020 automated adsorption system to obtain the BET surface areas and cumulative pore volumes of the catalysts.

The X-ray diffraction patterns were recorded on a Scintag XDS 2000 diffractometer using Cu Kα radiation. Scans were collected from 2-theta of 5° to 90° at a rate of 2° min^{-1}.

The DRIFTS experiments were carried out in a Harrick Praying Mantis accessory on a Bio-Rad FTS-60A FT-IR spectrometer. A sample was first mixed with KBr powder (75 wt.% KBr, 25 wt.% sample) and loaded into the DRIFTS cell. Scans were recorded after heating to 773 K in flowing dinitrogen for 1 h and cooling to ambient temperature. Carbon dioxide (purified by 3 Å molecular sieves) was introduced to the cell at 30 cm^3 min^{-1} for a total of 30 s. In a second set of experiments, anhydrous methanol was introduced to the cell by saturating a flowing N_2 stream at 40 cm^3 min^{-1} and flowing the gas mixture over the sample for 15 min. After purging the cell with N_2, 100 scans of adsorbed CO_2 or CH_3OH were recorded at a resolution of 2 cm^{-1}. A temperature programmed experiment included heating the sample to various temperatures between 303 and 473 K in flowing N_2 and cooling to ambient temperature to acquire spectra.

Adsorption microcalorimetry experiments were carried out on the same home built instrument that has been described previously by Bordawekar et al. [31]. The instrument is a heat flow calorimeter with two cells that are inserted into a large aluminum block maintained at 303 K. One cell functioned as a sample cell and the other one served as a reference. A catalyst sample was first heated to 773 K for 3 h under vacuum to a pressure less than 10^{-2} Pa. The sample was then cooled and allowed to thermally equilibrate with the system for 2 h prior to adsorption of carbon dioxide. Initial dosing pressures of carbon dioxide ranged from 10 to 600 Pa, and each dose was allowed to equilibrate with the sample for 15 min.

2.3. Transesterification

The catalytic transesterification reactions were conducted in a round bottom flask at 333 K with an overhead stirrer. The reactor was equipped with a reflux condenser and was continuously purged with flowing N_2 at 40 cm^3 min^{-1}. Unless otherwise indicated, methanol (Fisher, 99.9%) and tributyrin (Acros 98%) were used as reactants. In each run, 136.5 g (4.25 mol) of methanol and 43.8 g (0.14 mol) of tributyrin were loaded into the reactor with 6.5 g (0.5 mol) of dibutyl ether (Aldrich, 99.3%) as an internal standard. After the temperature of the reactants reached 333 K, 0.5–1 g of the catalyst, which was first heat treated at 773 K for 1 h in flowing purified N_2, was added to the reactants to initiate the transesterification. After thermal pretreatment, the catalyst was directly transferred to the reactor to avoid CO_2 contamination from air. Liquid samples were removed from the reactor at different time intervals and analyzed for products using the same procedure described in previous work by Xi and Davis [8].

Some reaction tests were conducted with purified tributyrin to fully exclude the deactivation due to the possible carboxylic acid impurities from the tributyrin source. To obtain purified tributyrin, a mixture of 100 ml tributyrin and 40 ml saturated sodium carbonate aqueous solution (23.5 wt.%) was vigorously stirred for 20 h at room temperature. Then the mixture was allowed to settle and the organic layer was separated. Approximately 16 g of 3A molecular sieves activated at 773 K were added to the organic layer and the mixture was allowed to remain at room temperature overnight. After the tributyrin was separated from the molecular sieves, vacuum distillation was performed to obtain purified tributyrin. In some cases, anhydrous methanol (Aldrich, 99.8%) was used as reactant. The purified reactants were tested in this reaction and had no observable effect on the activity of the mixed oxide catalysts.

Table 1
Influence of trace sodium on the conversion of tributyrin and yield of methylbutyrate over ZrO_2-P.

Sodium concentration wt.% (ppm)	Tributyrin conversion[a] (%)	Methylbutyrate yield[b] (%)
3.4 (34,000)	99.9	95.2
0.19 (1900)	6.7	2.2
0.01 (100)	0	0

[a] Reaction conditions: 1.00 g ZrO_2-P, T = 333 K, time = 2.66 h.
[b] Methylbutyrate yield is defined as the moles of MB produced divided by the moles of TB reacted divided by 3 (since three moles of MB are produced per mole of TB at complete conversion).

To test the effect of catalyst recycling on activity, the used catalyst was separated from the product solution by centrifugation and washed with 200 ml methanol prior to charging back into the reactor with fresh reactants.

Possible leaching was tested by separating the catalyst from the reaction mixture by centrifugation, at approximately 50% conversion. The liquid reactants were reinserted into the reactor and evaluated for any additional conversion.

The transesterification of tributyrin (T) with methanol (M) proceeds in three consecutive steps as shown in the following reaction sequence:

$$T + M \xrightarrow{k_1} D + MB \quad (1)$$

$$D + M \xrightarrow{k_2} Mo + MB \quad (2)$$

$$Mo + M \xrightarrow{k_3} G + MB \quad (3)$$

where D, MB, Mo and G denote dibutyrin, methyl butyrate, monobutyrin and glycerol, respectively. The reaction was assumed to be essentially irreversible and pseudo first order because of the large of excess of methanol. The pseudo first order kinetic model with respect to the butyrin components was used here to quantify the reaction rate constants on a surface area basis k_1, k_2, k_3 ($l\,mol^{-1}\,m^{-2}\,min^{-1}$) and the deactivation parameter α (min^{-1}) [8].

3. Results and discussion

3.1. Influence of trace sodium

The effect of washing the precipitated catalysts on the resulting level of trace sodium was investigated. A ZrO_2-P catalyst was first washed with 1 l of water. This sample had a residual loading of Na equal to 3.4 wt.% and was very active in the transesterification reaction (Table 1). A second ZrO_2-P catalyst was prepared in the same way except that it was washed with 5 l of water. The resulting catalyst had only 0.19 wt.% Na and a trace level of activity in transesterification. A third sample washed with 20 l of water had only 100 ppm of Na remaining on the catalyst. This zirconia sample had no perceptible activity for the transesterification under our standard conditions. The results from elemental analysis and reactivity tests are summarized in Table 1. These experiments confirmed that a pure zirconia sample is ineffective for transesterification of tributyrin with methanol at 333 K and that washing with 20 l of water was needed to remove sodium to levels that would not contribute to the transesterification reaction on the metal oxide surface. All further results presented are for catalysts that have been washed with 20 l of deionized water and have levels of Na that are negligible.

3.2. Comparison of Mg:Zr mixed oxides prepared by co-precipitation and sol–gel synthesis

Fig. 1 compares the X-ray diffraction pattern of a Mg:Zr-P catalyst with a molar ratio of 11:1 to those of MgO-P and ZrO_2-P. The

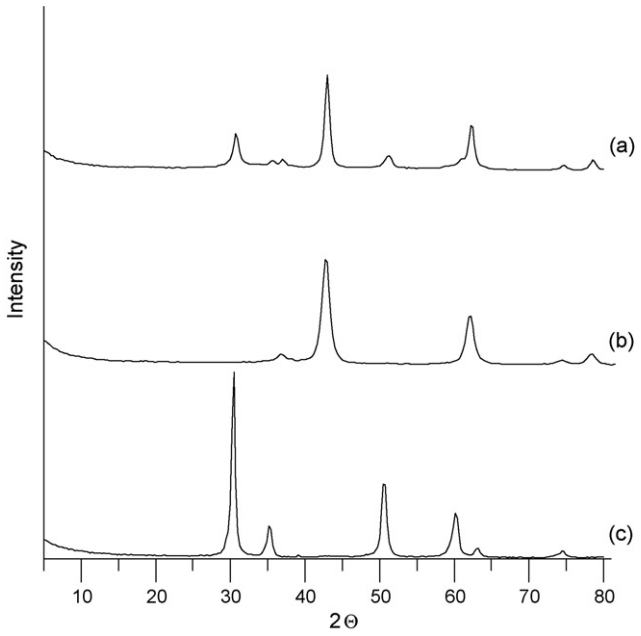

Fig. 1. Representative X-ray diffraction patterns of catalysts prepared by precipitation. (a) Mg:Zr-P 11:1, (b) MgO-P, and (c) ZrO_2-P. Patterns are offset for clarity.

MgO-P and ZrO_2-P were exclusively in the periclase and tetragonal forms, respectively. The co-precipitated mixed oxide exhibited diffraction peaks associated with both periclase MgO and tetragonal ZrO_2. In general, co-precipitated mixed oxides consisted of a mixture of both pure oxide crystals.

Fig. 2 compares a similar set of diffraction patterns for materials prepared by sol–gel synthesis. In this case, pure ZrO_2-SG had diffraction features associated with both the tetragonal and monoclinic (indicated by arrows) phases. Magnesia prepared by the sol–gel route was in the periclase form, consistent with the precipitated sample. The diffraction pattern of the 5:1 Mg:Zr-SG mixed oxide had very low intensity, broad features associated with periclase MgO. No crystalline form of ZrO_2 was detected. Evidently, sol–gel synthesis results in a sample that was better mixed at the atomic level, thus preventing crystallization of the individual oxides.

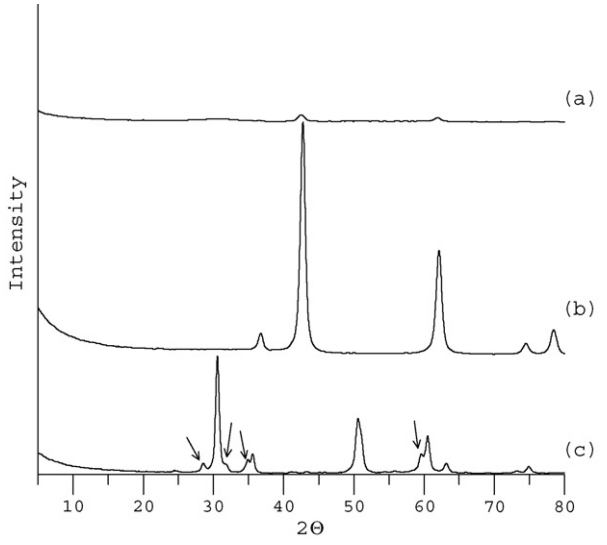

Fig. 2. Representative X-ray diffraction patterns of catalysts prepared by sol–gel synthesis. (a) Mg:Zr-SG 5:1, (b) MgO-SG, and (c) ZrO_2-SG (arrows indicate monoclinic ZrO_2). Patterns are offset for clarity.

Table 2
Surface areas and transesterification rate constants for catalysts prepared by precipitation and co-precipitation.

Catalyst	Surface area ($m^2\ g^{-1}$)	Cumulative pore volume ($cm^3\ g^{-1}$)	Catalyst loading (g)	k_1 ($\times 10^6$)[a] ($l\ mol^{-1}\ m^{-2}\ s^{-1}$)	k_2 ($\times 10^6$)[a] ($l\ mol^{-1}\ m^{-2}\ s^{-1}$)
Mg:Zr-P 1:1 (1.4)[b]	176	0.23	0.87	0.37 ± 0.12	0.34 ± 0.15
Mg:Zr-P 5:1 (5.6)[b]	223	0.22	0.75	0.50 ± 0.03	0.39 ± 0.09
Mg:Zr-P 8:1 (8.2)[b]	256	0.24	0.75	0.73 ± 0.07	0.75 ± 0.22
Mg:Zr-P 11:1 (11.1)[b]	173	0.56	0.82	3.00 ± 0.30	3.57 ± 0.85
MgO-P	292	0.46	0.90	0.70 ± 0.02	0.90 ± 0.07
MgO from $Mg(OH)_2$[c]	22	–	0.70	1.16 ± 0.34	1.19 ± 0.67
ZrO_2-P	123	0.12	1.00	0	0
MgO:ZrO_2-P 11:1[d]	–	–	1.00	1.19 ± 0.31	0.96 ± 0.41

[a] Errors represent 95% confidence intervals on fitted reaction rate constants.
[b] Values in parentheses indicate Mg/Zr molar ratio from elemental analysis.
[c] $Mg(OH)_2$, nanopowder (Aldrich, 99.9%).
[d] A physical mixture of MgO-P and ZrO_2-P in a Mg:Zr 11:1 molar ratio.

Table 3
Surface areas and transesterification rate constants for catalysts prepared by the sol–gel method.

Catalyst	Surface area ($m^2\ g^{-1}$)	Cumulative pore volume ($cm^3\ g^{-1}$)	Catalyst loading (g)	k_1 ($\times 10^6$)[a] ($l\ mol^{-1}\ m^{-2}\ s^{-1}$)	k_2 ($\times 10^6$)[a] ($l\ mol^{-1}\ m^{-2}\ s^{-1}$)
Mg:Zr 1:1-SG (0.96)[b]	118	0.27	0.83	0	0
Mg:Zr 5:1-SG (5.4)[b]	120	0.41	0.50	0.32 ± 0.08	0.43 ± 0.77
MgO-SG	134	0.37	0.74	0.87 ± 0.08	0.74 ± 0.16
ZrO_2-SG	120	0.11	1.00	0	0

[a] Errors represent 95% confidence intervals on fitted reaction rate constants.
[b] Values in parentheses indicate Mg/Zr molar ratio from elemental analysis.

A typical reaction profile for the transesterification of tributyrin with methanol over a mixed oxide catalyst is presented in Fig. 3. The lines in the figure are the results from the fitting procedure used with the experimental points. The rate constants derived from the fitting procedure are used to compare the reaction rates over the various materials.

The rate constants for transesterification of tributyrin with methanol over a series of mixed oxides prepared by co-precipitation are compared to those associated with the pure oxides in Table 2. The simplest way to compare specific activity is to examine the rate constant for the consumption of tributyrin as characterized by k_1. In every case the rate constant for dibutyrin conversion to monobutyrin, represented by k_2, confirmed the activity ranking by tributyrin loss. Since the rate of monobutyrin consumption to form glycerol during the sequential reaction could not be reliably quantified (the glycerol level was very low through most of the reaction), it was not reported. The rate constants were normalized by the exposed surface areas determined by N_2 adsorption.

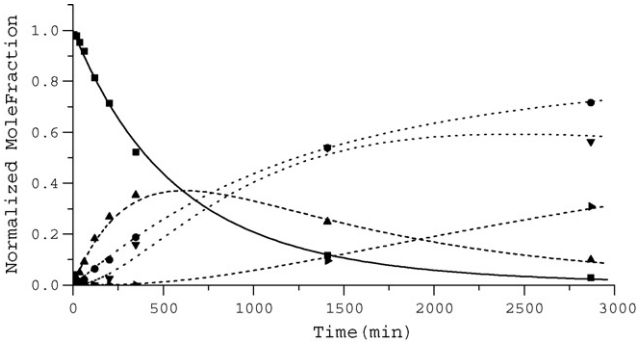

Fig. 3. Reaction profile from transesterification of tributyrin with methanol at 333 K over 5:1 Mg:Zr-P mixed oxide. The lines are obtained by fitting the model to the experimental data points. The concentrations are normalized to initial tributyrin concentration, where methylbutyrate is divided by 3. (■) Tributyrin, (▲) dibutyrin, (▼) monobutyrin, (►) glycerol, and (●) methylbutyrate.

The results in Table 2 illustrate the effect of Zr on the reactivity of Mg-rich mixed oxides. Two important conclusions can be drawn from the results. First, decreasing the amount of Zr increased the activity of the mixed oxide for transesterification. Second, a mixed oxide with Mg:Zr-P ratio of 11:1 was 300% more active than pure MgO-P, on a surface area basis. This finding was unusual, but was repeated by re-synthesizing and retesting the mixed oxide catalyst. Moreover, MgO prepared from calcination of $Mg(OH)_2$ exhibited essentially the same activity as MgO-P, although the surface areas of the two MgO samples varied by more than an order of magnitude. As discussed earlier, ZrO_2 was inactive for transesterification under our standard conditions. Moreover, a physical mixture of MgO-P and ZrO_2-P in a ratio of 11:1 converted tributyrin at a rate similar to that of pure MgO-P (Table 2).

The rate constants for transesterification over a series of catalysts prepared by sol–gel synthesis are summarized in Table 3. As mentioned above, ZrO_2 was not active. The activity of MgO-SG (Table 3) was similar to that formed by precipitation or calcination of commercial $Mg(OH)_2$ (Table 2). A 1:1 Mg:Zr-SG ratio was not active for transesterification, which contrasts the result from 1:1 Mg:Zr-P. Presumably, the atomic level mixing of Mg and Zr as achieved by the sol–gel method was detrimental to base catalysis. The rates observed over the 5:1 Mg:Zr mixed oxides were similar, but less than that of pure MgO. Apparently the synthesis method was not a critical parameter at high Mg contents. Unfortunately, we could not successfully prepare a mixed oxide catalyst with a high ratio of Mg:Zr (11:1) by the sol–gel route.

The re-usability of the most active catalyst (11:1 Mg:Zr-P) was also tested. The catalyst was removed by centrifugation, washed with methanol and used for two subsequent reactions. The conversion of tributyrin and the yield of methylbutyrate for each reaction are presented in Table 4. On the basis of tributyrin conversion, the catalyst retained 85% and 75% of its original activity after the first and second recycles, respectively.

A mixed oxide was evaluated for leaching by removal of the catalyst in the middle of the reaction and checking for additional conversion in the reactant mixture. Fig. 4 shows the reaction profile after removing a Mg:Zr-P 8:1 catalyst at about 180 min. Although there was some conversion of tributyrin after centrifugation, the

Table 4
Recycle experiments for transesterification on Mg:Zr-P 11:1.

Reaction[a]	Tributyrin conversion[b] %	Methylbutyrate yield[c] %
1	84	52
2	72	39
3	61	25

[a] Run 1 is for fresh catalyst whereas subsequent runs are after centrifugation and methanol washing.
[b] Reaction conditions: 0.79 g 11:1 Mg:Zr-P, T = 333 K, time = 22 h.
[c] Methylbutyrate yield is defined as the moles of MB produced divided by the moles of TB reacted divided by 3.

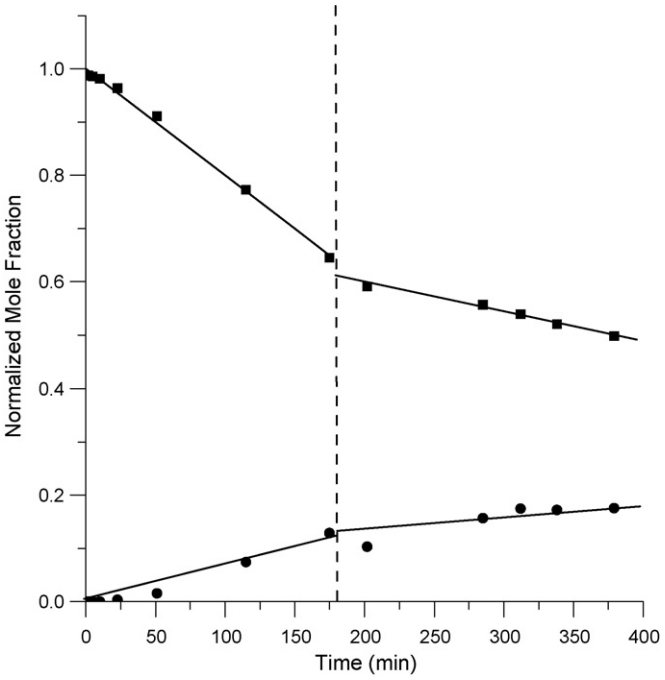

Fig. 4. Reaction profile from transesterification of tributyrin with methanol at 333 K over 8:1 Mg:Zr-P mixed oxide. The concentrations are normalized to initial tributyrin concentration, where methylbutyrate is divided by 3. The dashed vertical line at approximately 180 min corresponds to the removal of the catalyst by centrifugation. (■) Tributyrin and (●) methylbutyrate.

majority of the rate was attributed to the solid catalyst. The small level of conversion after catalyst removal could be attributed to either a small amount of leaching or incomplete removal of small catalyst particles by centrifugation.

3.3. DRIFTS of adsorbed CO_2 and CH_3OH

Since the Mg-rich mixed oxide (Mg:Zr-P 11:1) was substantially more active than MgO-P, we attempted to characterize the nature of its surface by FT-IR spectroscopy of adsorbed CO_2 and

Table 5
Representative structures of adsorbed carbon dioxide and methanol [32–40].

Designation	Carbon dioxide adsorption mode	Methanol adsorption mode
I	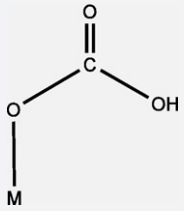	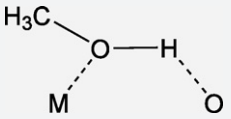
II	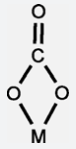	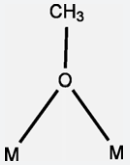
III	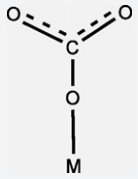	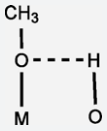

CH_3OH. Carbon dioxide adsorption on basic oxides has been typically described by three different adsorption modes, bicarbonate, bidentate, and unidentate. Table 5 presents the schematic representations of these adsorbate structures and Table 6 summarizes the wavenumber positions of features typically associated with each mode. Each of the adsorption modes in Table 5 has asymmetric and symmetric O–C–O vibration modes. As indicated in Table 6, the bicarbonate structure also exhibits a C–OH bending mode. Fig. 5 compares the DRIFTS of CO_2 on the pure oxides MgO-P and ZrO_2-P as well as on the highly-active 11:1 Mg:Zr-P mixed oxide. In the spectra associated with MgO-P, three different types of carbonate were detected. The intensities of the IR features decreased with increasing temperature as CO_2 desorbed from the surface. The features that disappeared first appear to originate from bicarbonate; for example, one of the bicarbonate peaks at 1225 cm^{-1} was absent after heating to 373 K. The bands associated with bidentate and unidentate carbonate remained in the spectra of CO_2 on MgO-P even after heating to 473 K. Interestingly, these features appeared to be more intense on the mixed oxide sample. Moreover, the DRIFTS confirmed the same features of CO_2 on both magnesia and zirconia.

Since DRIFTS of adsorbed CO_2 did not reveal an obvious structural modification of the Mg:Zr-P mixed oxide surface, we explored the adsorption of CH_3OH. This molecule is a logical choice because it was a reagent in the transesterification reaction. In this case, significant differences were observed in the DRIFTS of CH_3OH on the

Table 6
Representative values for the IR shifts for carbon dioxide adsorption in the range of 1200–1800 cm^{-1} [32–37].

	ν_{as} OCO (cm^{-1})[a]	ν_s OCO (cm^{-1})[b]	ν COH (cm^{-1})[c]
Bicarbonate (MgO)	1646–1650	1405–1480	1220–1225
Bidentate (MgO)	1610–1691	1320–1362	N/A
Unidentate (MgO)	1360–1405	1510–1560	N/A
Bicarbonate (t-ZrO_2)[d]	1620	1450	1225–1230
Bidentate (t-ZrO_2)[d]	1550–1570	1325–1350	N/A
Unidentate (t-ZrO_2)[d]	1425–1430	1450–1460	N/A

[a] Asymmetric O–C–O stretching vibration.
[b] Symmetric O–C–O stretching vibration.
[c] COH bending mode only associated with bicarbonate.
[d] t-ZrO_2 is tetragonal zirconia.

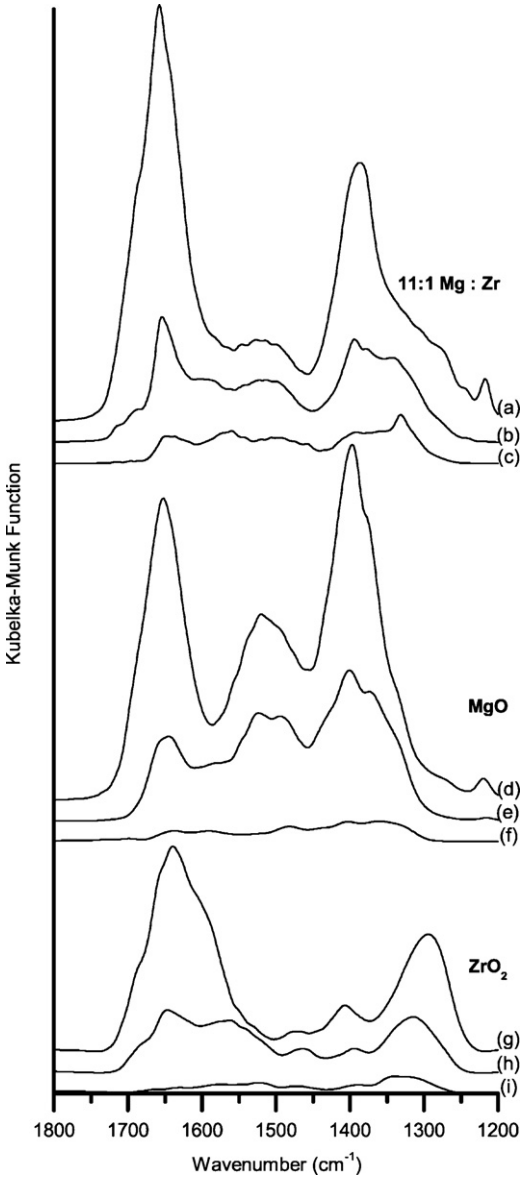

Fig. 5. DRIFT spectra after adsorption and stepwise desorption of CO_2. Spectra (a), (b) and (c) are associated with CO_2 on Mg:Zr-P 11:1 after heating to 303, 373 and 473 K, respectively, and cooling to 303 K. Spectra (d), (e) and (f) are associated with CO_2 on MgO-P after heating to 303, 373 and 473 K, respectively, and cooling to 303 K. Spectra (g), (h) and (i) are associated with CO_2 on ZrO_2-P after heating to 303, 373 and 473 K, respectively, and cooling to 303 K. Spectra are offset for clarity.

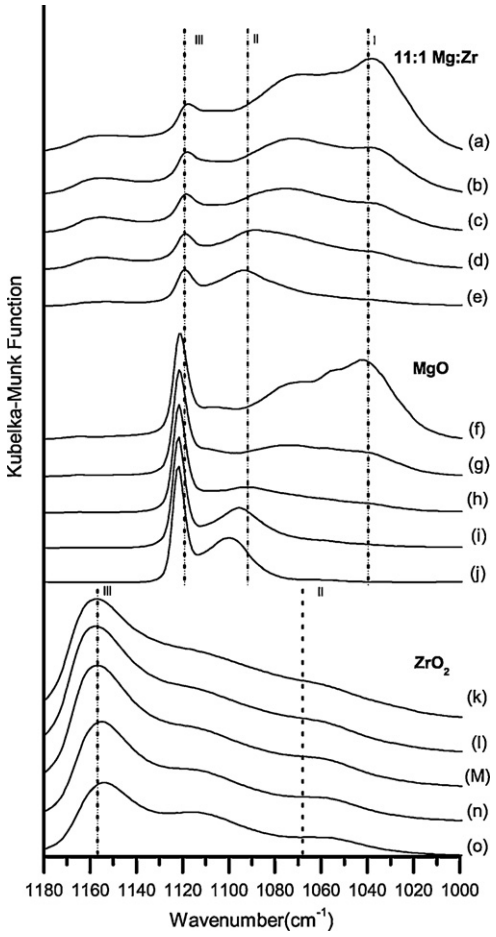

Fig. 6. DRIFT spectra after adsorption and stepwise desorption of CH_3OH. Spectra (a), (b), (c), (d), and (e) are associated with CH_3OH on Mg:Zr-P 11:1 after heating to 303, 333, 373, 423 and 473 K, respectively, and cooling to 303 K. Spectra (f), (g), (h), (i) and (j) are associated with CH_3OH on MgO-P after heating to 303, 333, 373, 423 and 473 K, respectively, and cooling to 303 K. Spectra (k), (l), (m), (n) and (o) are associated with CH_3OH on ZrO_2-P after heating to 303, 333, 373, 423 and 473 K, respectively, and cooling to 303 K. Spectra are offset for clarity.

catalysts. Tables 5 and 7 summarize the various modes of adsorbed CH_3OH and the positions of the IR features associated with those modes, respectively. The DRIFTS for CH_3OH on the representative catalyst samples are presented in Fig. 6. Zirconia appears to have the largest relative amount of methanol adsorbed in the deprotonated form (Type III, Table 5) but the bands are broader and shifted in position to higher wavenumbers from the type III features on MgO-P and the Mg:Zr-P mixed oxide. The MgO-P and Mg:Zr-P 11:1 samples have three modes of CH_3OH adsorption: molecularly-adsorbed (type I), bidentate (type II), and unidentate (type III). The unidentate and bidentate forms appears to be fairly stable since they were observed on the surface after heating to 473 K. Although the mixed oxide and magnesia had similar features in the DRIFTS of CH_3OH, the relative intensity of the bidentate mode compared to the unidentate mode was higher on the mixed oxide. Moreover, the IR spectra of methanol adsorbed on a physical mixture of MgO-P and ZrO_2-P in a ratio of 11:1 revealed features that were nearly identical to the spectra associated with MgO-P in Fig. 6. At this point, we cannot state whether any of these structures are relevant to the transesterification reaction of tributyrin with methanol.

Table 7
Representative values for the IR vibration modes for methanol adsorption in the range of 1200–1000 cm^{-1} [38–40].

	ν H_3C–O (cm^{-1})[a]
Molecularly-adsorbed (MgO)	1033–1060
Bidentate (MgO)	1500–1920
Unidentate (MgO)	1090–1115
Bidentate (t-ZrO_2)[b]	1070
Unidentate (t-ZrO_2)[b]	1154

[a] C–O vibrations of adsorbed methanol.
[b] t-ZrO_2 is tetragonal zirconia.

3.4. CO_2 adsorption microcalorimetry

Fig. 7 presents the CO_2 adsorption isotherms obtained from the adsorption microcalorimetry experiments. The total CO_2 capacity was derived from extrapolating the saturation portion of the isotherm to zero pressure as depicted by the solid lines in the plots. Although the uptakes were similar on the materials (1–2 μmol CO_2 m^{-2}), ZrO_2-P had the largest adsorption capacity,

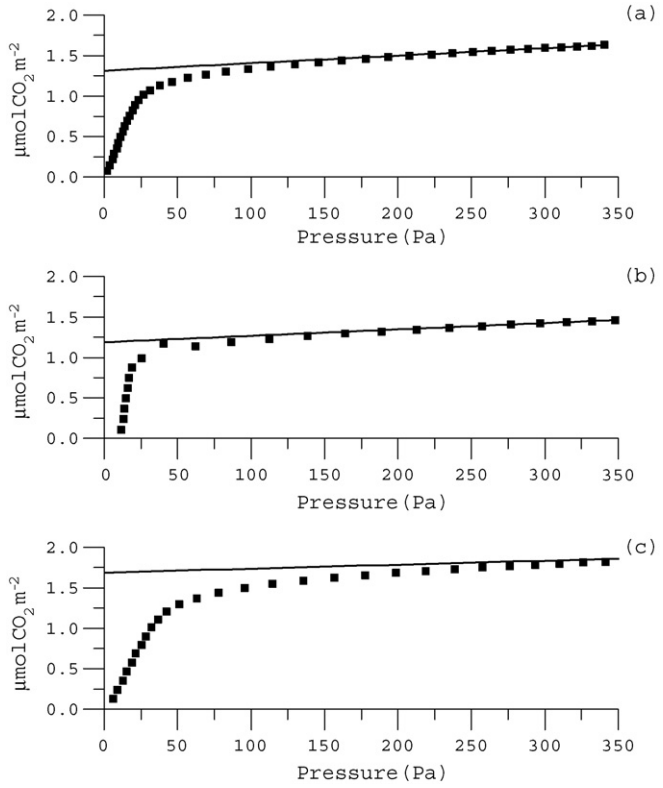

Fig. 7. Representative CO_2 adsorption isotherms, on (a) Mg:Zr-P 11:1, (b) MgO-P, and (c) ZrO_2-P prepared by precipitation obtained from the microcalorimetry experiment. The lines represent the extrapolation of saturation conditions to zero pressure to obtain the total CO_2 adsorption capacity.

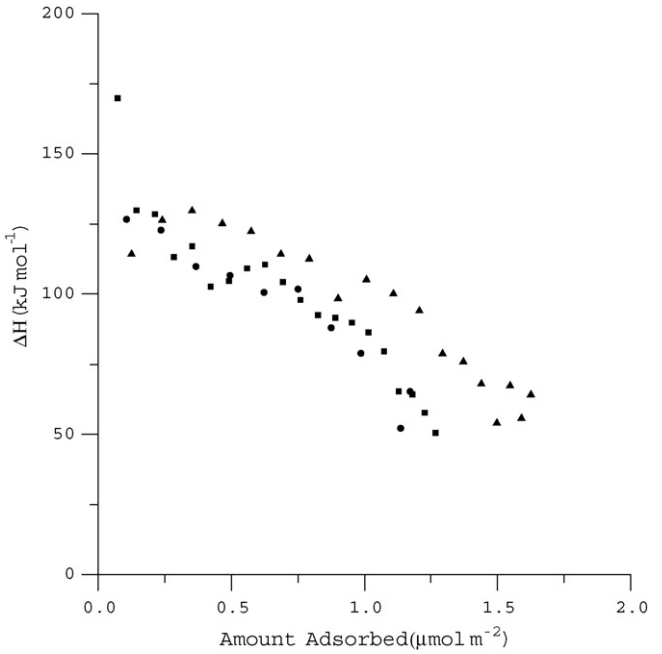

Fig. 8. Heat of CO_2 adsorption as a function of the amount adsorbed, normalized by surface area, on samples prepared by precipitation. (■) Mg:Zr-P 11:1, (●) MgO-P, and (▲) ZrO_2-P.

followed by the Mg:Zr-P 11:1 mixed oxide, and MgO-P. A comparison of the CO_2 uptakes as summarized in Table 8 to the rate constants presented in Table 2 indicates that there is no correlation between the CO_2 capacity and the activity for transesterification. This is rather surprising since CO_2 is often used as a measure of surface basicity.

Fig. 8 compares the heat of adsorption as a function of CO_2 adsorption on the precipitated materials. The initial heat of adsorption represented by the first point at low coverage is reported in Table 8 along with the heat of adsorption at a surface coverage equal to half the saturation coverage. As with CO_2 adsorption capacity, there was no apparent correlation of the heat of CO_2 adsorption with the catalytic activity. However, it is interesting to note that the highest initial heat of adsorption (170 kJ mol^{-1}) was associated with the mixed oxide with the greatest catalytic activity. More work is needed to understand the role of the strongest of basic sites on the catalytic activity. One hypothesis for the exceptional activity of the 11:1 Mg:Zr-P mixed oxide is that a few basic sites with a high affinity for CO_2 are created by adding small amounts of Zr to MgO. The rest of the surface appears to expose sites similar to those on MgO-P, according to DRIFTS of CO_2 and CH_3OH.

These results suggest that perhaps a minor fraction of modified surface adsorption sites might account for the promotional effect of Zr on catalysis by MgO. These special minority sites could be located at grain boundaries between the Mg and Zr oxide crystallites. Recent work by Vidruk et al. suggests that modification of grain boundaries in MgO creates strong base sites that are responsible for an approximately 4-fold increase in activity for transesterification [41]. Altered grain boundaries could explain the results we obtained for Mg:Zr-P 11:1 mixed oxide. Modified MgO-like base sites were observed by CO_2 adsorption microcalorimetry, DRIFTS of adsorbed methanol, and enhanced transesterification activity. Extensive characterization work is needed to confirm this idea.

3.5. Comparison to a mixed oxide of Ti and Mg

Mixed oxides of magnesia and titania have also been reported to exhibit enhanced surface basicity compared to pure MgO [16,26]. Therefore, a mixed oxide prepared by precipitation of Mg onto TiO_2 with a Mg:Ti ratio of 14:1 was synthesized and determined to have a k_1 for transesterification of 0.4 l mol^{-1} m^{-2} s^{-1} with a surface area of 293 m^2 g^{-1}. This observed rate was approximately 50% of that associated with pure MgO-P on a surface area basis. A mixed oxide of Mg:Ti-SG ratio of 3:1 was also synthesized. Results from X-ray diffraction of the calcined material failed to reveal any crystalline phases. This sol–gel derived catalyst as well as pure titania obtained from precipitation, sol–gel synthesis, and Evonik (Aeroxide P25) were inactive for transesterification at our standard conditions.

Table 8
Summary of results from CO_2 adsorption microcalorimetry on Mg and Zr oxide samples, prepared by precipitation.

Catalyst	Catalyst loading (g)	CO_2 uptake (µmol m^{-2})	Initial heat of adsorption (kJ mol^{-1})	Heat at 1/2 saturation (kJ mol^{-1})
Mg:Zr-P 1:1 (1.4)[a]	0.14	1.6	145	117
Mg:Zr-P 5:1 (5.6)[a]	0.13	1.2	154	126
Mg:Zr-P 8:1 (8.2)[a]	0.16	1.0	154	106
Mg:Zr-P 11:1 (11.1)[a]	0.20	1.3	170	104
MgO-P	0.12	1.2	127	101
t-ZrO_2-P	0.30	1.7	114	98

[a] Values in parentheses indicate Mg/Zr molar ratio from elemental analysis.

4. Conclusions

Mixed oxides of magnesia and zirconia have great potential for base catalyzed reactions. First, mixed oxides prepared by sol–gel synthesis were better mixed at the atomic level since the X-ray diffraction patterns revealed poor crystallinity compared to samples prepared by co-precipitation. However, the only significant promotional effect for transesterification was observed on a magnesia-rich mixed oxide (Mg:Zr-P 11:1) prepared by co-precipitation. The X-ray pattern of this sample revealed phases of both MgO and ZrO_2, suggesting that perhaps the promotional effect occurred at the interface between phases. The influences of trace sodium and catalyst leaching on activity were ruled out by control experiments. In an attempt to relate surface properties to catalysis, DRIFTS of adsorbed CO_2 and CH_3OH were recorded on the most active mixed oxide, standard MgO-P and inactive ZrO_2-P. The DRIFTS of adsorbed CO_2 was not effective at distinguishing between the samples. However, DRIFTS of adsorbed CH_3OH showed very significant differences among the samples. Although the mixed oxide sample was primarily composed of magnesia, the DRIFTS of CH_3OH showed a different ratio of unidentate to bidentate modes. Moreover, the initial heat of CO_2 adsorption on the mixed oxide was greater than that on MgO-P. Initial attempts to promote magnesia with Ti were unsuccessful.

Acknowledgement

This work was supported by the Chemical Sciences, Geosciences and Biosciences Division, Office of Basic Energy Sciences, Office of Science, U.S. Department of Energy, grant no. DE-FG02-95ER14549.

References

[1] M. Di Serio, M. Ledda, M. Cozzolino, G. Minutillo, R. Tesser, E. Santacesaria, Ind. Eng. Chem. Res. 45 (2006) 3009.
[2] M. Diasakou, A. Louloudi, N. Papayannakos, Fuel 77 (1998) 1297.
[3] J.V. Gerpen, Fuel Process Technol. 86 (2005) 1097.
[4] F. Ma, M.A. Hanna, Bioresour. Technol. 70 (1999) 1.
[5] A.C. Pinto, L.L.N. Guarieiro, M.J.C. Rezende, N.M. Ribeiro, E.A. Torres, W.A. Lopes, P.A.D. Pereira, J.B. de Andrade, J. Braz. Chem. Soc. 16 (2005) 1313.
[6] F. Figueras, M.L. Kantam, B.M. Choudary, Curr. Org. Chem. 10 (2006) 1627.
[7] N. Barakos, S. Pasias, N. Papayannakos, Bioresour. Technol. 99 (2008) 5037.
[8] Y. Xi, R.J. Davis, J. Catal. 254 (2008) 190.
[9] G. Vicente, M. Martinez, J. Aracil, Bioresour. Technol. 92 (2004) 297.
[10] Z. Shi, L. Xu, S. Da, Y. Feng, Microporous Mesoporous Mater. 94 (2006) 34.
[11] D.E. López, J.G. Goodwin Jr., D.A. Bruce, E. Lotero, Appl. Catal. A Gen. 295 (2005) 97.
[12] A.L. Mckenzie, C.T. Fishel, R.J. Davis, J. Catal. 138 (1992) 547.
[13] C.T. Fishel, R.J. Davis, Catal. Lett. 25 (1994) 87.
[14] E.J. Doskocil, S.V. Bordawekar, R.J. Davis, J. Catal. 169 (1997) 327.
[15] M.A. Aramendía, V. Borau, C. Jiménez, J.M. Marinas, J.R. Ruiz, F.J. Urbano, Appl. Catal. A Gen. 244 (2003) 207.
[16] M.A. Aramendía, V. Borau, C. Jiménez, A. Marinas, J.M. Marinas, J. Navio, J.R. Riz, F.J. Urbano, J. Mol. Catal. A Chem. 218 (2004) 81.
[17] J. Li, R.J. Davis, Appl. Catal. A Gen. 239 (2003) 59.
[18] M. Tu, R.J. Davis, J. Catal. 199 (2001) 85.
[19] L.C. Meher, D. Vidya Sagar, S.N. Naik, Renew. Sust. Energy Rev. 10 (2006) 248.
[20] T. Yamaguchi, Catal. Today 20 (1994) 199.
[21] M.A. Aramendía, V. Borau, C. Jiménez, J.M. Marinas, A. Porras, F.J. Urbano, J. Catal. 161 (1996) 829.
[22] R. Sree, N. Seshu Babu, P.S. Sai Prasad, N. Lingiaiah, Fuel Process. Technol. 90 (2009) 152.
[23] M.L. Rojas-Cervantes, L. Alonso, J. Díaz-Terán, A.J. López-Peinado, R.M. Martín-Aranda, V. Gómez-Serrano, Carbon 42 (2004) 1575.
[24] J.N. Chheda, J.A. Dumesic, Catal. Today 123 (2007) 59.
[25] C.J. Barrett, J.N. Chheda, G.W. Huber, J.A. Dumesic, Appl. Catal. B Environ. 66 (2006) 111.
[26] M.A. Aramendía, V. Borau, C. Jiménez, A. Marinas, J.M. Marinas, J. Navio, J.R. Riz, F.J. Urbano, Colloids Surf. A 234 (2004) 17.
[27] D. Ciuparu, A. Ensuque, F. Bozon-Verduraz, Appl. Catal. A Gen. 326 (2007) 130.
[28] H. Gocmez, H. Fujimori, Mater. Sci. Eng. B 148 (2008) 226.
[29] S. Liu, X. Zhang, J. Li, N. Zhao, W. Wei, Y. Sun, Catal. Commun. 9 (2008) 1527.
[30] T. Settu, Ceram. Int. 26 (2000) 517.
[31] S.V. Bordawekar, E.J. Doskocil, R.J. Davis, Langmuir (1998) 1734.
[32] D. Bianchi, T. Chafik, M. Khalfallah, S.J. Teichner, Appl. Catal. A Gen. 112 (1994) 219.
[33] V. Bolis, G. Magnaca, G. Cerrato, C. Morterra, Thermochim. Acta 379 (2001) 147.
[34] B. Bachiller-Baeza, I. Rodriguez-Ramos, A. Guerrero-Ruiz, Langmuir 14 (1998) 3556.
[35] J.I. Cosimo, V.K. Diez, M. Vu, E. Iglesia, C.R. Apesteguia, J. Catal. 178 (1998) 499.
[36] V.K. Diez, C.R. Apesteguia, J.I. Cosimo, Catal. Today 63 (2000) 53.
[37] G.A.H. Mekhemer, S.A. Halawy, M.A. Mohamed, M.I. Zaki, J. Phys. Chem. C 108 (2009) 13379.
[38] M. Bailly, C. Chizallet, G. Costentin, J. Krafft, H. Lauron-Pernot, M. Che, J. Catal. 235 (2005) 413.
[39] K.T. Jung, A.T. Bell, Top. Catal. 20 (2002) 97.
[40] F. Khairallah, A. Glisenti, J. Mol. Catal. A Chem. 274 (2007) 137.
[41] R. Vidruk, M.V. Landau, M. Herskowitz, M. Talianker, N. Frage, V. Ezersky, N. Froumin, J. Catal. 263 (2009) 196.